

AD-A241 157



2

MASSACHUSETTS INSTITUTE OF TECHNOLOGY  
ARTIFICIAL INTELLIGENCE LABORATORY

A.I. Memo No. 1216

December 1990

**Causes and Effects of Chaos**

**Elizabeth Bradley**

DTIC  
ELECTE  
OCT 07 1991  
S D

**Abstract**

Most of the recent literature on chaos and nonlinear dynamics is written either for popular science magazine readers or for advanced mathematicians. This paper gives a broad introduction to this interesting and rapidly growing field at a level that is between the two. The graphical and analytical tools used in the literature are explained and demonstrated, the rudiments of the current theory are outlined and that theory is discussed in the context of several examples: an electronic circuit, a chemical reaction and a system of satellites in the solar system.

**91-12378**



Copyright © Massachusetts Institute of Technology, 1990

This report describes research done at the Artificial Intelligence Laboratory of the Massachusetts Institute of Technology. Support for the laboratory's artificial intelligence research is provided in part by the Advanced Research Projects Agency of the Department of Defence under Office of Naval Research contracts N00014-85-K-0124 and N00014-86-K-0180.

This document has been approved  
for public release and sale; its  
distribution is unlimited.

| REPORT DOCUMENTATION PAGE  |   |  | Form Approved<br>OMB No. 0704-0188         |  |
|--|---|--|--|--|
| Public reporting burden for this collection of information is estimated to average 1 hour per response, including the time for reviewing instructions, searching existing data sources, gathering and maintaining the data needed, and completing and reviewing the collection of information. Send comments regarding this burden estimate or any other aspect of this collection of information, including suggestions for reducing this burden, to Washington Headquarters Services, Directorate for Information Operations and Reports, 1215 Jefferson Davis Highway, Suite 1204, Arlington, VA 22202-4302, and to the Office of Management and Budget, Paperwork Reduction Project (0704-0188), Washington, DC 20503. |   |  |  |  |
| 1. AGENCY USE ONLY (Leave blank)   | 2. REPORT DATE<br>December 1990                             | 3. REPORT TYPE AND DATES COVERED<br>memorandum             |  |  |
| 4. TITLE AND SUBTITLE<br>Causes and Effects of Chaos   |   | 5. FUNDING NUMBERS<br>N00014-85-K-0124<br>N00014-86-K-0180 |  |  |
| 6. AUTHOR(S)<br>Elizabeth Bradley  |   |  |  |  |
| 7. PERFORMING ORGANIZATION NAME(S) AND ADDRESS(ES)<br>Artificial Intelligence Laboratory<br>545 Technology Square<br>Cambridge, Massachusetts 02139  |   | 8. PERFORMING ORGANIZATION<br>REPORT NUMBER<br>AIM 1216    |  |  |
| 9. SPONSORING / MONITORING AGENCY NAME(S) AND ADDRESS(ES)<br>Office of Naval Research<br>Information Systems<br>Arlington, Virginia 22217  |   | 10. SPONSORING / MONITORING<br>AGENCY REPORT NUMBER        |  |  |
| 11. SUPPLEMENTARY NOTES<br>None  |   |  |  |  |
| 12a. DISTRIBUTION / AVAILABILITY STATEMENT<br>Distribution of this document is unlimited   |   |  | 12b. DISTRIBUTION CODE                     |  |
| 13. ABSTRACT (Maximum 200 words)<br><br>Most of the recent literature on chaos and nonlinear dynamics is written either for popular science magazine readers or for advanced mathematicians. This paper gives a broad introduction to this interesting and rapidly growing field at a level that is between the two. The graphical and analytical tools used in the literature are explained and demonstrated, the rudiments of the current theory are outlined and that theory is discussed in the context of several examples: an electronic circuit, a chemical reaction and a system of satellites in the solar system.  |   |  |  |  |
| 14. SUBJECT TERMS (key words)<br>dynamical systems      nonlinear systems<br>chaos   |   |  | 15. NUMBER OF PAGES<br>44                  |  |
|  |   |  | 16. PRICE CODE<br>\$4.00                   |  |
| 17. SECURITY CLASSIFICATION<br>OF REPORT<br>UNCLASSIFIED   | 18. SECURITY CLASSIFICATION<br>OF THIS PAGE<br>UNCLASSIFIED | 19. SECURITY CLASSIFICATION<br>OF ABSTRACT<br>UNCLASSIFIED | 20. LIMITATION OF ABSTRACT<br>UNCLASSIFIED |  |

# Causes and Effects of Chaos

Elizabeth Bradley

Department of Electrical Engineering and Computer Science  
Massachusetts Institute of Technology

December 14, 1990

## Abstract

Most of the recent literature on chaos and nonlinear dynamics is written either for popular science magazine readers or for advanced mathematicians. This paper gives a broad introduction to this interesting and rapidly growing field at a level that is between the two. The graphical and analytical tools used in the literature are explained and demonstrated, the rudiments of the current theory are outlined and that theory is discussed in the context of several examples: an electronic circuit, a chemical reaction and a system of satellites in the solar system.

|               |              |
|---------------|--------------|
| Accession For |              |
| NTIS          | CRAS         |
| DTIC          | IAS          |
| Unannounced   |              |
| Justification |              |
| By            |              |
| Distribution  |              |
| Availability  |              |
| Dist          | Availability |
| A-1           |              |

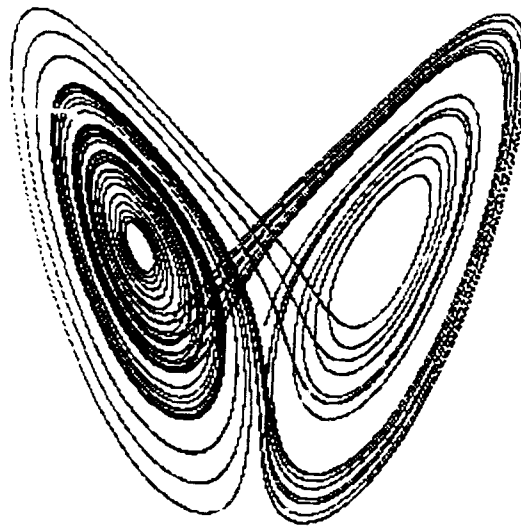


Figure 1: Lorenz Attractor

## 1 Introduction

Chaos is complicated, unpredictable and seemingly random behavior in a deterministic physical system. A system need not be complex, noisy or subject to experimental error to exhibit chaotic behavior: it need only be nonlinear. This flouts the classic conception of determinism as expressed by Laplace: “given the exact position and velocity of every particle in the universe, [I can] predict the future for the rest of time” [3]. This view is not only unrealistic but actually untrue. Two objects at starting points separated by a distance smaller than can be measured can follow vastly different paths through space. Another important revelation about chaos is its universality. In the throes of chaos, many different systems, from fluids to economics to the human heart, act alike.

Chaos was first discovered in turbulent fluid flow, considered “the” unsolved problem in classical physics[5]. Fluid flow turns from smooth (laminar) to turbulent as its velocity increases. The classic explanation for this [22] was that new frequencies appeared, one at a time, in the velocity and density profiles. In the early 1960s, a meteorology professor at MIT named Edward Lorenz simulated the actions of an air mass between warm ground and cool clouds, modeled by a simplified version of the Navier-Stokes equations for fluid flow[23]. The system traced out a never-repeating and yet highly structured path in its phase space (pressure versus velocity,) as shown in figure 1. If the classic scenario were correct, the pattern would eventually have repeated itself. Lorenz also recognized the underlying cause — the non-linearity in the Navier-Stokes equations maps small causes into huge effects.

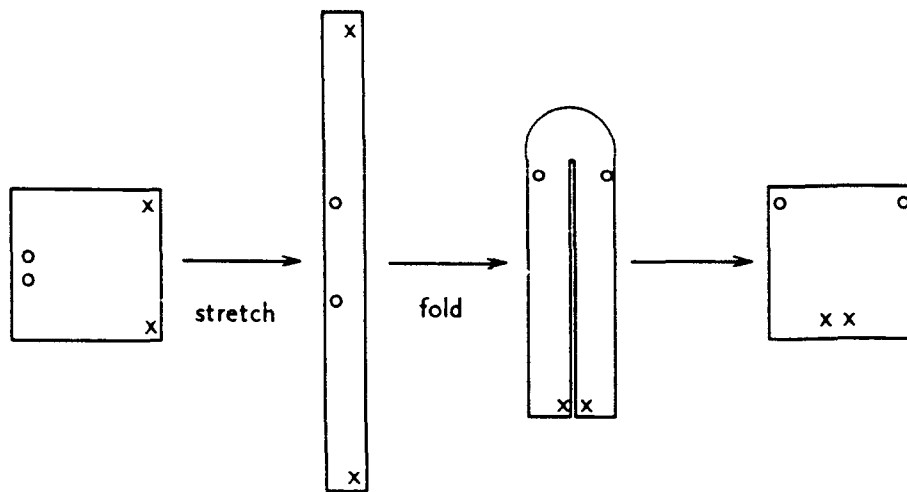


Figure 2: Smale's Horseshoe

This was later termed the “Butterfly Effect”: a butterfly stirring the air today in Peking can transform storm systems next month in New York[12]. In the late 1960s and early 1970s, researchers in many different fields rediscovered chaos, unaware of results that had been published in other fields' journals<sup>1</sup>. After much proselytizing by the Dynamical Systems Collective at UC Santa Cruz (distinguished by their use of an analog computer as well as by their early interest in the field) and others, cross-fertilization took place in the mid 1970s and the study of chaos and nonlinear dynamics has been gaining momentum ever since. The intricate, beautiful patterns of nonlinear dynamics, brought out by the graphics in various glossy books[25, 26], has recently captured public interest, much as the universality of the theory has aroused scientific interest.

Mathematically, the definition [6] of chaotic behavior requires: (1) sensitive dependence upon initial conditions (2) topological transitivity and (3) dense periodic points in the Poincaré section of the system's state space. Sensitive dependence is illustrated by Smale's horseshoe, the nonlinear transformation shown in figure 2. The points marked with os start close together and finish far apart; the points marked with xs do the opposite. A *linear* transformation, such as the stretch which performs the first part of the horseshoe transformation, scales all distances in the same direction. The nonlinearity — the folding — makes sensitive dependence possible and also

<sup>1</sup>“Communication across the revolutionary divide is inevitably partial” [21].

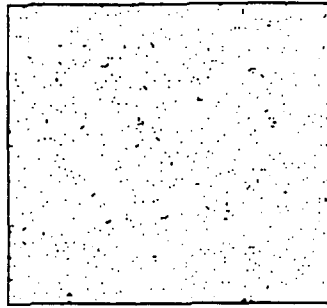


Figure 3: Close-Up View



Figure 4: Global View

keeps the figure bounded in space. This gives a flavor of unpredictability to the behavior, although only deterministic forces are present. A system in a chaotic regime is random in the sense that the future cannot be predicted without an infinite-precision knowledge of the present. A truly random process can only be described in terms of average properties, whereas a chaotic process is fully described by a (often quite simple) nonlinear equation. It can be hard to tell the difference, especially in experimental data. Presented with figure 3, a small section of a system's phase space that looks like an evenly distributed cloud of dots, it is impossible to determine whether the system is random or chaotic. However, on a larger scale (as in figure 4,) some structure might take form, indicating that the system is not really random<sup>2</sup>. Topological transitivity means that chaotic regions are connected: chaotic trajectories are confined to one region unless perturbed. Chaotic and non-chaotic regions — any number of each — can peacefully coexist, sometimes intricately intertwined, on a system's phase space. Periodic orbits in a system's state space appear as periodic points on a section of that space. This apparently orderly behavior seems out of place within the chaos, let alone as part of its definition; almost all of these orbits, however, exert no influence

---

<sup>2</sup>The same structure might appear within the apparent randomness in Figure 3 if more data points were included; see the discussion of fractals later in this section.

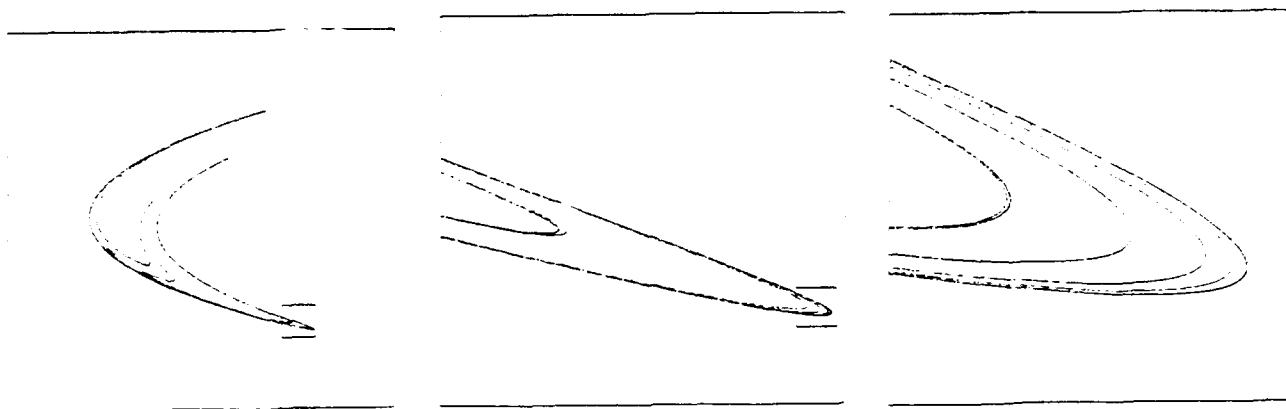


Figure 5: Series of Expansions

because they are unstable<sup>3</sup>. These three criteria for chaos are commonly but by no means universally agreed upon.

Although nonlinearity has been positively identified as a *necessary* condition for chaotic behavior, *sufficient* conditions (in real physical systems) are not as clear. The usefulness of this body of knowledge is thus limited since one cannot, in general, predict where it will apply. Some *symptoms* have, however, been identified. When a system's characteristic period suddenly doubles, one should suspect chaos. Repeated doublings make the diagnosis more sure. Chaos' patterns of "structured randomness" on phase space plots are very distinctive. Formal, mathematical evidence is sparse: "the justification for classifying much irregular behavior as chaos depends on the accumulation of numerical evidence and on experience with a few idealized mathematical systems known to [have positive Lyapunov exponents]"[20]. These difficulties often lead papers in this field to take intuitive, informal approaches to definitions, causes and effects. Chaos has reduced strict theorists to classifying "clues" and stating that one outcome is more "likely" than another. The highly intuitive understanding that such descriptions engender is wonderful, but the informality can be frustrating at times.

A fractal [25] is a structure which looks the same under different power magnifying glasses. The series of expansions in figure 5 shows this *scaling* property. A cross section of this structure is a version of the Cantor set, a line segment with the middle third removed *ad infinitum*: The Hausdorff

<sup>3</sup>External control has been used to stabilize systems at some of these periodic points [15].

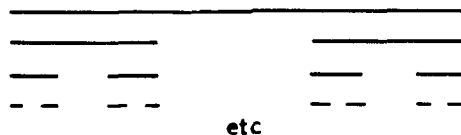


Figure 6: Cantor Set

dimension of a set is strictly less than the topological dimension of the manifold on which it lives and need not be an integer. For the Cantor set in figure 6, which is neither a point nor a line, the Hausdorff dimension  $d_h$  is 0.63. For a Cantor set with the middle fifth removed,  $d_h = 0.76$ . A fractal is a set that has fractional Hausdorff dimension. Fractal structure is common in nature; examples are the bronchi in the human lung and branches on trees. Perhaps the most striking example of this type of object is the Mandelbrot set. Beautiful photos of various types of fractals can be found in [26].

Fractals play a role in the universality of chaos: many chaotic systems show fractal structure in their phase diagrams. In fact, figure 5 shows iterations of the system of nonlinear difference equations:

$$\begin{aligned} x_{n+1} &= \alpha - x_n^2 + \beta y_n \\ y_{n+1} &= x_n \end{aligned} \quad (1)$$

with  $\alpha = 1.24$  and  $\beta = 0.4$ . The pattern we see is called the Hénon attractor. The map models, among other things, the patterns of a dripping faucet. See Appendix B.

Since researchers have been alerted to its form, chaos' distinctive patterns have been observed in many physical systems — often in previously discounted, “noisy” data. Chaos can explain noise that doesn't act quite right, that has some hints of structure. Some of the patterns of the approach of chaos have been identified, which could allow it to be diverted or encouraged, as desired. “Sensitive dependence on initial conditions” creates a wealth of structure from simple system equations, which suggests a new approach to describing complex structures or encoding information. Despite its proponents' almost-religious fervor, however, chaos theory does not solve every outstanding problem in dynamics.

One severe drawback of the theory is its lack of necessary and sufficient conditions. Another is the relationship between parts and whole. For example, figure 3 can be constructed from figure 4, but the converse is not true in general. Conflicts with thermodynamics also arise. Cream stirred into a cup of coffee is a good example of this — the equations governing interac-



tion of the spoon and the small volume elements of fluid are deterministic and yet the mixing sends the system down the (unclimbable, by the second law of thermodynamics) entropy hill. Chaos theory says that the process is reversible *in principle*, but that any tiny slip of the spoon will scotch it. The paradox may eventually be reconciled if the "tiny slips" are proved to be unavoidable. It is also difficult to reconcile chaos and quantum mechanics; this is part of the bigger problem that the latter has with the world as it is portrayed in classical mechanics. Schrödinger's equation is linear. Because it describes the fundamental constituents of matter, one should theoretically be able to use quantum mechanics to describe anything at all, but the linearity theoretically precludes any chaotic behavior!

The rest of this document is organized as follows. One section is devoted to each of four papers from the current literature and one section to a summary. The first paper describes a body of theory and the next three describe applications of that theory to different physical systems: an electronic circuit, a chemical reaction, and a system of satellites in the solar system.

## 2 Theory

Lagrangians can be used to write  $2N$  first-order differential equations describing any  $N$  degree-of-freedom system; such a system has a  $2N$ -dimensional state space. If the system is linear, solving the equations is a matter of linear algebra. A simple harmonic oscillator is an example of this type of system:

$$\begin{aligned}\frac{dx}{dt} &= y \\ \frac{dy}{dt} &= -x\end{aligned}\tag{2}$$

Nonlinear equations are harder, and often impossible, to solve in closed form. The simple pendulum's equations:

$$\begin{aligned}\frac{d\theta}{dt} &= \omega \\ \frac{d\omega}{dt} &= -\frac{g}{l} \sin \theta\end{aligned}\tag{3}$$

which reduce to a scaled version of the system (2) if  $\theta \ll 1$ , can be solved in closed form using elliptic functions<sup>4</sup> but this tractability is unusual. Most nonlinear systems, like the Van der Pol oscillator in appendix A, whose equations are:

$$\begin{aligned}\frac{dx}{dt} &= y \\ \frac{dy}{dt} &= -(x + ay - by^3)\end{aligned}\tag{4}$$

must be integrated numerically. Confronted with such equations, one tries to find *constants of the motion*, such as energy or momentum. Each such constant can be used to reduce, by substitution, the number of equations that remain to be solved; finding  $2N$  of them solves the system completely. Systems in which this holds are described as *integrable*. System trajectories then follow curves of constant energy, angular momentum, etc<sup>5</sup>. Many mathematical tricks have been developed to aid in finding these useful quantities;

---

<sup>4</sup>In fact, elliptic functions were invented to solve this problem

<sup>5</sup>If the Hamiltonian  $H$  is time-independent — that is, if potential and kinetic energy are functions only of positions and velocities — then  $H$  itself is a constant of the motion.

see, for example, [13, page 55] and the discussion of Lyapunov exponents later in this section.

Chaos can only arise in nonlinear systems, but not all nonlinear systems are chaotic — only those that are non-integrable[16]. Non-integrable equations are often well-behaved for some parameter (coefficient) values and chaotic for others. Only a very few nonlinear problems — the simple pendulum and the two-body problem, for example — have integrable equations, so one need not look far to find a chaotic system. Finding out what parameter values push the system over the edge may not be so easy.

Three dimensions are required for chaos in continuous time systems, but only one is needed for chaos in iterated maps; this implies, among other things, that a *double* pendulum has enough degrees of freedom to be chaotic, whereas a single pendulum does not (unless it is driven.) Chaotic maps fold manifolds, forcing trajectories to cross over each other. The uniqueness theorem causes an obvious problem with this in 2-space, but an extra dimension allows trajectories to cross over one another without touching (which would cause one starting point to have two future solutions.) Iterated solutions escape this requirement because they define time in clicks, changing the definition of “at the same time” — essentially, a crossing-over point can hide between snapshots.

In a review paper[8], Eckmann treats non-integrable systems that “are well understood for some value of the control parameter” and that mutate from order to chaos as the parameter is changed. He also restricts discussion to dissipative systems, for reasons discussed in the next paragraph. System evolution equations are presented either in the form of equations (1), for iterated maps, or in the form of the systems (2), (3) or (4) for continuous-time systems.

An attractor is a region in phase space into which all trajectories within some larger enclosing region converge. In figure 7,  $W$  is the attractor and  $V$  is the “basin of attraction” (cf. the Atlantic ocean and the terrain east of the continental divide.) The formal definition also requires  $W$  to be indecomposable (i.e., in one piece.) Attractors appear once transients have died out. An attractor can be a fixed point (like  $v_C = 0, i_L = 0$  in an RLC circuit), a limit cycle (a sine wave generator), an  $n$ -torus ( $n$  signal generators generating a Lissajous figure on an  $n$ -input oscilloscope), or something much more complex, like the Lorenz attractor in the introduction. Most non-dissipative systems, like LC circuits, have closed orbits. These aren't attractors because they don't vacuum up nearby trajectories. Liouville's theorem states this formally: non-dissipative or *conservative* mappings preserve the volume of phase space. Only dissipative mappings, which contract phase space, can have attractors.

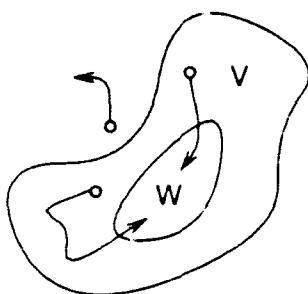


Figure 7: Definition of an Attractor

The definition of a *strange attractor*, one of the phase space signatures of a chaotic system, has one additional clause, embodying “sensitive dependence upon initial conditions.” Eckmann’s definition differs in tone from the rest of the literature, including the writings of the men who discovered [23] and named [29] strange attractors. He points out (rightly) that “although [the dissipative map] contracts volumes, it need not contract lengths”, and follows this reasoning to the conclusion: “points which are arbitrarily close initially may get macroscopically separated on the attractor after sufficiently large time intervals.” In direct contrast, other authors [14, 29] emphasize that the time intervals need not be large at all. Helleman notes a 16 order-of-magnitude change “after a short time[16].” All of these statements suffer from an ill-defined notion of “large” and “small” in regard to time; the time scales of sensitive dependence are discussed further at the end of section 2. As was the case with the definition of chaos, there are as many (slightly different) definitions of strange attractors as there are authors writing about them. One of the most popular identifies strange attractors as those with fractional Hausdorff dimension.

As mentioned in the first paragraph of this section, variations in equation parameters can change order into chaos. These variations can also alter the topology and texture of the phase space, making attractors change shape or size. Figure 8 shows a series of snapshots of the behavior of some typical system, taken at different times during the transformation from order to chaos. The left column is the time domain, the middle the frequency domain, and the right column a projection of the phase space (velocity against position). The value of the “nonlinearity parameter” is lowest at the top and highest at the bottom. The top two rows of graphs show period-one and period-two limit cycles and the bottom row shows the system after the onset of chaos. The attractor on the bottom right is aperiodic and the corresponding fre-

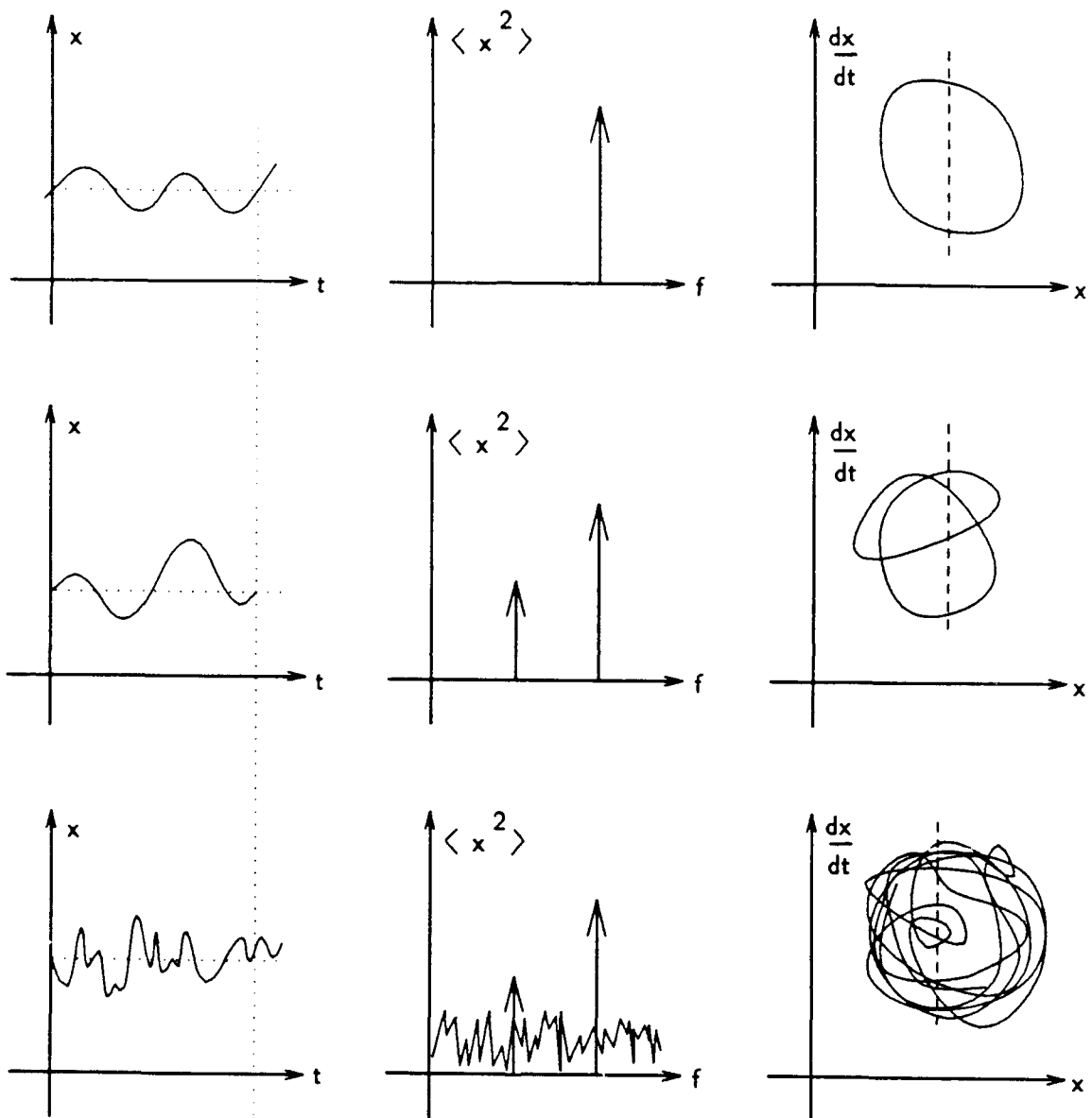


Figure 8: From Order to Chaos

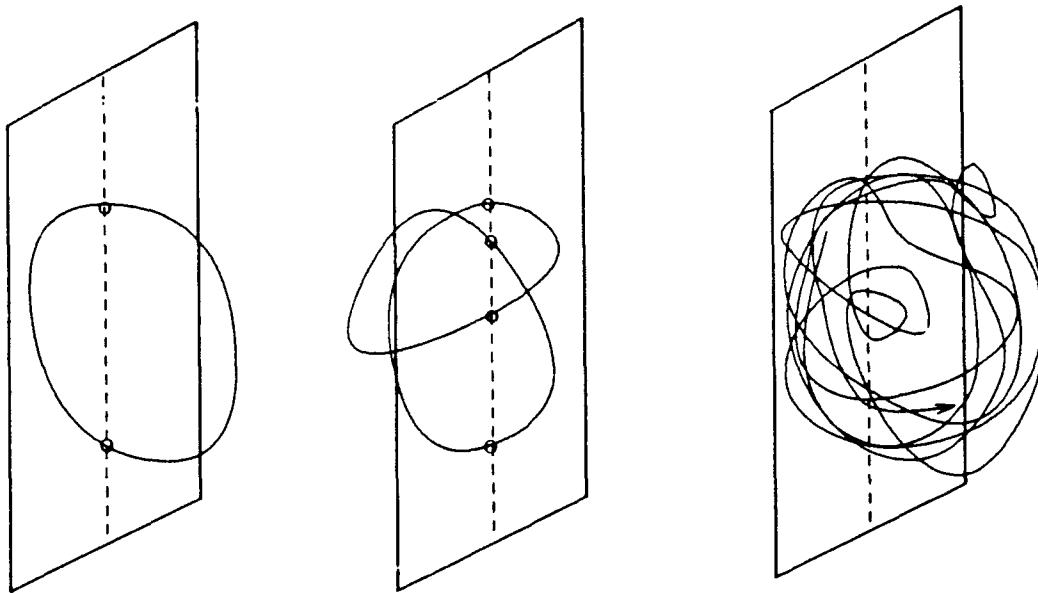


Figure 9: Poincaré Section

quency spectrum shows broad-band energy (which is in general not noise, or else it would have appeared on the two previous spectra, assuming identical conditions for all three experiments).

Two other graphical tools are extremely valuable — the Poincaré section and the bifurcation diagram. The former is an  $n - 1$  dimensional cross section of a region in  $n$  dimensional phase space. A two-dimensional Poincaré section of the trajectories in figure 8 is shown in figure 9. A bifurcation diagram, as in figure 10, is a stack of Poincaré sections (or projections thereof, to reduce the dimension and make the picture easier to understand), measured or computed at different values of the parameter. The three vertical lines in figure 10 correspond to the dashed lines in figures 8 and 9. On these axes, period doublings appear as pitchforks and chaos as dark bands of dots. The veiled lines within these bands correspond to areas of the Poincaré sections that cut through an attractor where its threads are dense. Note the windows of order in the chaotic region; a better picture [20, page 173] shows further period doublings within these windows. The merging of the chaotic bands is caused by topological changes in an attractor and is termed “reverse bifurcation.”

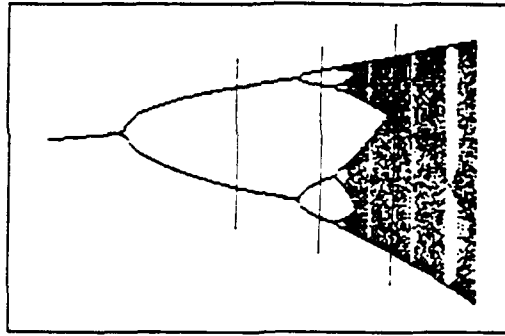


Figure 10: Bifurcation Diagram

The Lyapunov exponent is defined as:

$$\lambda = \lim_{N \rightarrow \infty} \frac{1}{N} \sum_{n=1}^N \ln \left( \left| \frac{dF}{dx}(x_n) \right| \right) \quad (5)$$

A function that has a negative  $\lambda$  in some region is said to be “stable in the sense of Lyapunov;” its trajectories are attracted to some proper subset of that region.  $\lambda$  measures how fast neighboring trajectories separate; a positive  $\lambda$  is an alternate definition of chaos. Note the correspondence between bands of chaos on the the bifurcation diagram in figure 10 and positive  $\lambda$ s on figure 11. The arrows indicate the parameter values marked by dashed lines on several previous figures. Zero  $\lambda$ s correspond to integrals of the motion, which can be practical: integrals for the Toda problem were found only after their existence was suggested by zero  $\lambda$ s in numerical data[11].

A correlation graph is a plot of  $x_n$  against its previous values. This is an ideal format in which to present data from, say, a dripping faucet, with the intervals between successive drops as the  $x_n$  [12, page 262], [3, page 55]. A regular, period-one flow looks like a single dot on such axes. A long/short interval pattern would be dots on two corners of a rectangle whose sides are the lengths of the intervals. For high flow rates a faucet’s drip rate becomes aperiodic, manifesting as a structured cloud of points on the correlation graph (in fact, the structure appears to be a variant of the Hénon attractor shown in the introduction and in appendix B.)

Eckmann uses these tools, with the exception of the Lyapunov exponent and the correlation diagram, and with the addition of the eigenvalues of the system’s Jacobian, evaluated on the fixed attractor, to classify system dynamics. He analyzes three scenarios, or “paths to chaos”, which a system can follow as a parameter is varied. This is *not* a standard scientific approach: *if* some conditions are met *then* other things are “likely” to happen. This

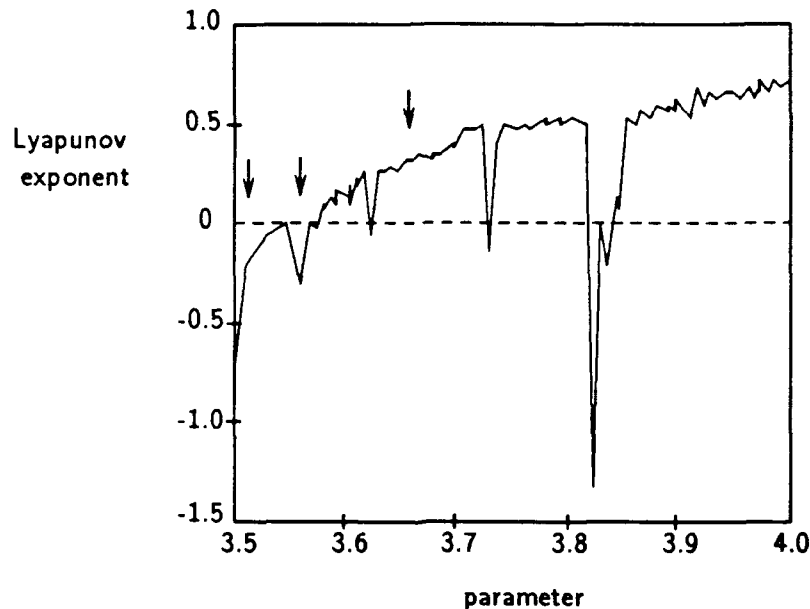


Figure 11: Lyapunov Exponent (after [20])

form of analysis capitulates to the unformed nature of chaos theory; it is very effective but it makes its author uncomfortable. A whole page — 10% of the paper — is devoted to disclaimers like: “The theory is completely general, but it cannot describe its domain of application” and “Results cannot be generalized.”

Each of the next three subsections analyzes one of these scenarios. For each case, the mathematical statement given in [8] is translated into English; its implications in an experimental setup are then assessed. The form of the characteristic *signature*, on at least one of the different plots given in section 1, is given for each. These signatures will be used in sections 3, 4 and 5 to classify data from the the three applications papers.

## 2.1 The Ruelle-Takens-Newhouse Scenario

A Hopf bifurcation occurs when a stable fixed point splits into a repelling fixed point and a stable limit cycle — the structure found in the phase diagram of a Van der Pol oscillator (see appendix A.) This transformation takes place when a pair of complex eigenvalues of the system’s Jacobian cross



the imaginary axis as the parameter changes. The frequency of the new limit cycle is *independent* of existing system frequencies.

Given this definition, the Ruelle-Takens-Newhouse scenario for the onset of chaos can be stated as follows: *if* a system undergoes three Hopf bifurcations and its vector field holds certain properties over a certain type of set, *then* the system possesses a strange attractor. This scenario is the oldest of the three and is omitted from many modern texts [6, 33].

Exact verification of this scenario requires knowledge of the exact equations that describe the system. This is realistic when one is simulating mathematical equations, but impossible for a physical system. " $C^2$  neighborhoods in Axiom A vector fields" are hard to identify in noisy, inaccurate experimental data, so some characteristics or clues must be distilled out of the description.

The signature of this scenario is the successive appearance, as the non-linearity is turned up, of up to three *independent* frequencies on the power spectrum, followed by the sudden onset of broad-band "noise" underneath the peaks, much like the spectrum on the bottom line of figure 8.

## 2.2 The Feigenbaum Scenario

The definition of the conditions that give rise to the Feigenbaum scenario is much more exact (and complicated) than that of the Ruelle-Takens-Newhouse scenario. The proof involves defining a space of functions and proving that the sequence  $f, f^2, f^4, \dots$  (the functions whose fixed points are cycles with period 1, 2, 4, ... — the bifurcation points of  $f$ ) converges. Feigenbaum's original paper [10] gives a simpler explanation and derivation based on scaling or renormalizing curves near fixed points. The complex proof alluded to above was developed later by Eckmann and others[4]. Again, this formalism is all moot; one cannot measure convergence on a function space for physical data. Feigenbaum concedes this point: "If [a flow exhibits period doubling], our theory applies. However, to prove that a given flow (or any flow) should exhibit doubling is well beyond present understanding. All we can do is experiment[10]."

The mathematical "if" part may be more complex than the previous scenario, but the clues that can be distilled from the "then" part are much more concrete and widely applicable. Feigenbaum systems undergo an infinite sequence of period-doubling bifurcations of stable periodic orbits (pitchfork bifurcations) at specific intervals of parameter and amplitude. In contrast to the previous scenario, there is only one independent frequency; all others

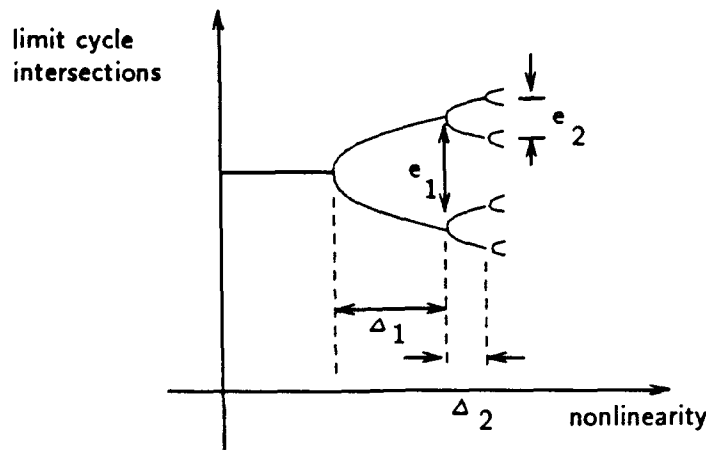


Figure 12: Feigenbaum's Scenario

are subharmonics. The intervals between bifurcations decrease steadily, parameterized by the constant  $\delta$ . The bifurcations thus get closer and closer, converging at the "accumulation point" or onset of chaos. See figure 12. Feigenbaum predicts, in the limit of large  $i$  and independent of the details of the system, within bounds<sup>6</sup>:

$$\frac{\Delta_i}{\Delta_{i+1}} = \delta = 4.6692\dots$$

$$\frac{e_i}{e_{i+1}} = \alpha = 2.5029\dots$$

This has been repeatedly verified in the literature, both numerically and with data from physical systems. The bifurcation diagram in figure 10 was obtained by iterating the logistic map, which originated in population modeling:

$$x_{n+1} = Kx_n(1 - x_n) \quad (6)$$

The horizontal axis is  $K$ . Values of  $K$ ,  $\delta$  and  $\alpha$  are shown in table 1 for the first three bifurcations.  $\alpha$  is given for the topmost set of branches on the tree. The  $\alpha$ s and  $\delta$ s aren't exactly 2.50.. and 4.66.. — those values hold only in the limit of large  $i$ . Detection of more bifurcations would require more decimal places for parameter specification and hence would become impossible at  $\frac{\text{bits}}{\log_2 10}$ , where *bits* is the number of bits used to store a floating

<sup>6</sup>This applies to any any function that can be approximated, near its maximum, as a parabola.

| Periods | $K$   | Interval | $\delta$ | $\alpha$ |
|---------|-------|----------|----------|----------|
| 2       | 3     | -        | -        | -        |
| 4       | 3.445 | 0.445    | -        | 2.424    |
| 8       | 3.542 | 0.097    | 4.588    | 2.107    |

Table 1: Measured Values for  $\delta$  and  $\alpha$

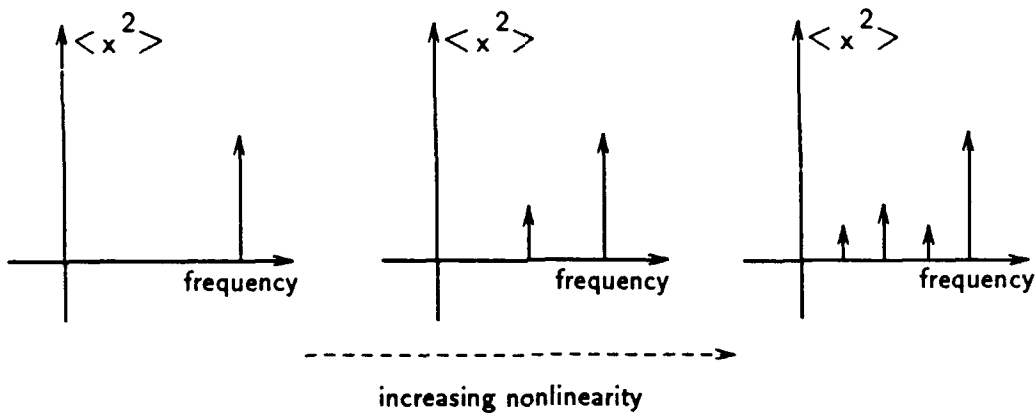


Figure 13: Feigenbaum's Scenario in the Frequency Domain

point number in the computer. This resolution limit affects observations as well as parameter specifications: the  $n^{\text{th}}$  bifurcation causes a "pitchfork" that is  $\alpha^{-n}$  wide and the computer deems differences below  $\frac{\text{bits}}{\log_2 10}$  to be invisible. These issues are discussed further in section 2.4.

On a frequency spectrum, as shown in figure 13, this scenario predicts that  $2^n$  spikes will appear, as the parameter increases, at the  $2^{-n}$ th subharmonics of the fundamental. A spectrum with an odd number of spikes, or with spikes at independent frequencies, would violate this condition (but might fit the Ruelle-Takens-Newhouse scenario.) Note that different scenarios could hold at the same time in different regions of phase space.  $\delta$  and  $e$  govern (respectively) the values of the parameter at which new spikes appear and their heights at each frequency. At the accumulation point, where the size of the bifurcation branches reaches zero, the chaotic regime begins. Eck-

mann contradicts himself in the description of the chaotic spectrum: "...one will observe aperiodic behavior, but no broad-band spectrum." Aperiodic behavior is usually thought of as broad-band. Frequency spectra which fit the Feigenbaum pattern have been found in many experiments. It is perhaps the most widely understood and accepted "path to chaos."

### 2.3 The Pomeau-Manneville Scenario

The statement of this scenario is the most qualitative and least mathematical of the three in Eckmann's paper. It is imprecise in that "there is no mention as to when the 'turbulent' regime is reached or what the exact nature of this turbulence is[8]." A "saddle-node" bifurcation occurs when two fixed points, one stable and one unstable, meet and annihilate one other. If such an event occurs, the system will exhibit "intermittently turbulent" behavior of random duration, interleaved with long stable periods. The length of these stable periods increases with the proximity of the two fixed points and is familiar to anyone who has ever trimmed an oscilloscope probe — the pole leaves a long, slow exponential tail on the step response.

This behavior is best illustrated on a "return map" — probably the most common expository device used in chaos articles in popular science magazines [3, 20]. For example, the equation

$$x_{n+1} = 1 - Rx_n^2 \quad (7)$$

describes a parabola in  $(x_{n+1}, x_n)$ -space. Repeated iterations can be graphically computed by drawing lines between the parabola and the 45 degree line (where  $x_{n+1} = x_n$ ), as shown in figure 14. This trajectory closes in on the fixed point along a squared-off spiral. If the nonlinearity ( $R$ ) is turned up, the parabola rears higher and its slope at the fixed point increases. When that slope reaches one, the point loses its stability and a pencil point bouncing between parabola and 45 degree line will find two fixed points: a bifurcation has taken place. The plots in figure 15 show the sequence of iterates for these two cases. The ordinate is iteration number ( $n$ ) and the abscissa is  $x_n$ . These data can also be plotted in *correlation form*, in  $(x_{n+1}, x_n)$ -space, as in figure 16. When  $R$  reaches 2, the system goes chaotic. The pencil point bounces all over the parabola and the iterates cover the range (figure 17.) Von Neumann actually used this particular mapping as a (not really very random) random number generator[5]. The clustered points correspond to the veiled lines in the bifurcation diagram and the clotted areas in the attractor. Seen on a return map, the iterates slowly cover the parabola.

If the parabola is close to the 45 degree line but does not touch it, the

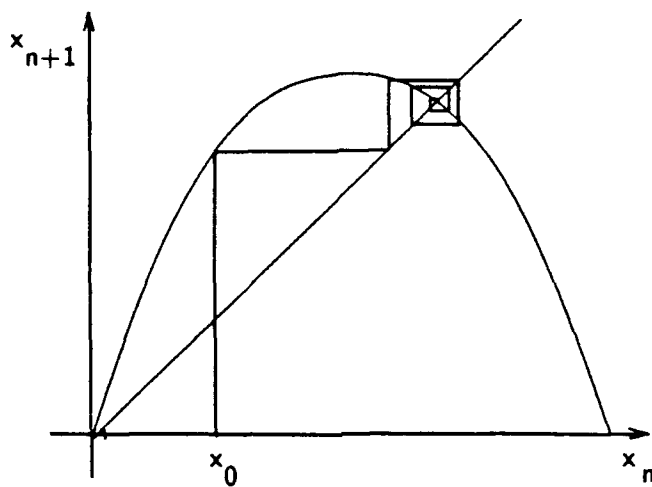


Figure 14: A Return Map for Equation (7)

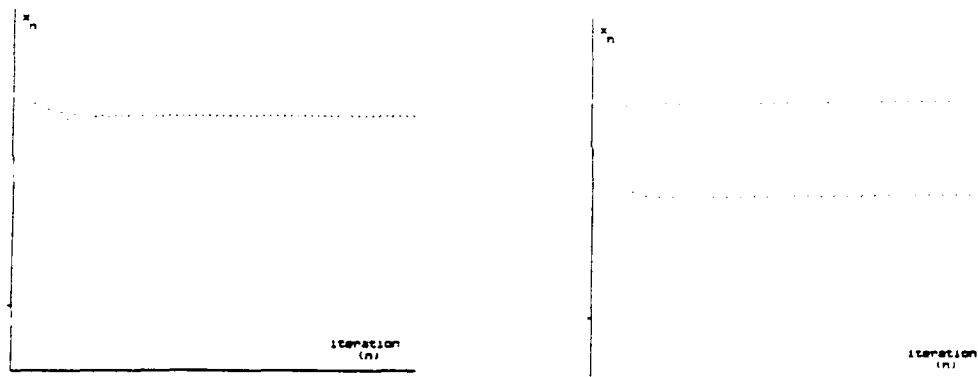


Figure 15: Iterates of Equation (7)

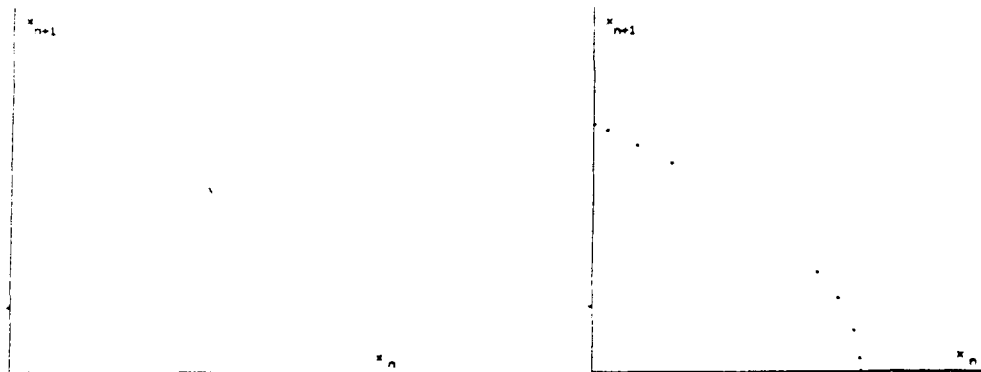


Figure 16: Iterates of Equation (7) in Correlation Form

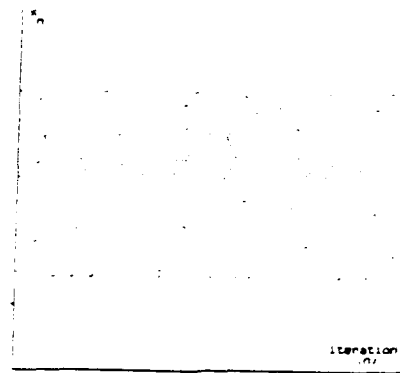


Figure 17: Chaotic Iteration Sequence

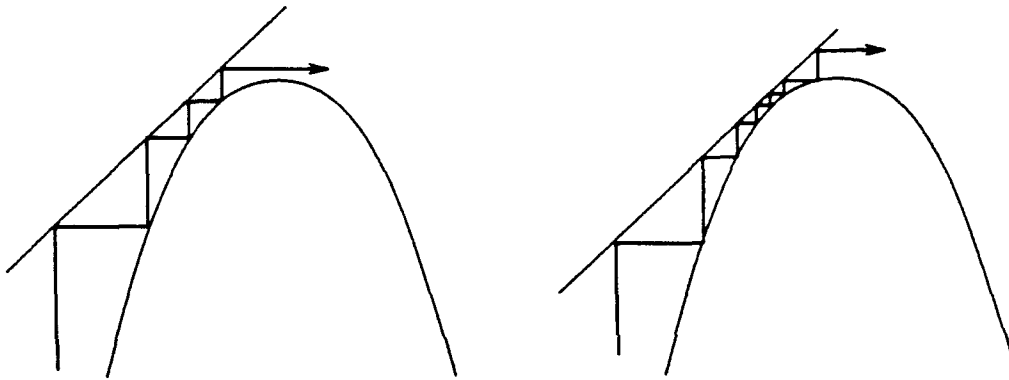


Figure 18: An Almost-Fixed Point

iterates appear to be converging to a fixed point, but then pass the point of closest approach and diverge, as in figure 18. If the distance between curve and 45 degree line is small, the system can appear to be at a fixed point for a while and then collapse into chaos. The smaller the distance, the longer the apparent stable orbit lasts. This transient stability appears in iterations of equation (7) as well as the logistic map — equation (6) — both upon entry to and exit from chaotic regions (Eckmann only discusses the onset of chaos). Iterates of equation (7) for parameter values just below a band of order within a chaotic zone are shown in figure 19. In these graphs, the system appears to be “trying to find” the same period-three solution from two slightly different starting points (20% and 21% of full scale). Note that the two sequences are very different, even at the beginning, despite the close starting values. The time constants of the tails seem to be the same in all “laminar” regions, but the duration of those regions varies. This is consistent with an iteration sequence entering one near-approach zone from

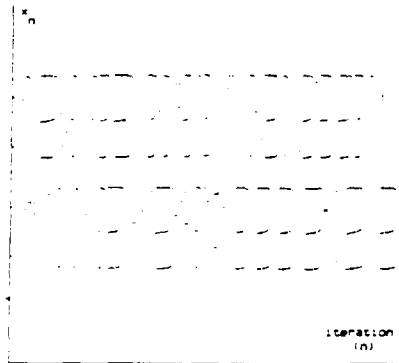


Figure 19: Mix of Periodic and Chaotic Behavior

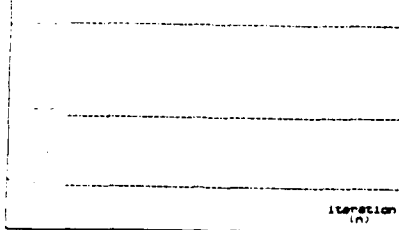


Figure 20: Convergence to Solutions

various paths<sup>7</sup>. If  $R$  is increased slightly, the parabola touches the 45 degree line. Iterations of this equation (figure 20) then converge to the solution that they seemed, in figure 19, to be seeking.

Eckmann points out several shortcomings of this scenario, some of which are caused by mathematical looseness. He found the reports of experimental data to be sparse and unconvincing. There are no defined long-range precursors to intermittency — the effects of the colliding fixed points are only felt when they approach each other. The Pomeau-Manneville scenario does not exclude the other two scenarios described. In fact, Feigenbaum uses the very same logistic map to illustrate his scenario[10]. Despite its drawbacks, this scenario does explain the perplexing regions of order in chaotic iteration sequences.

<sup>7</sup>Period-three cycles are significant for another reason: Sarkovskii's theorem states that if a one-dimensional iterated map has a period-three cycle, it will not only exhibit chaos but also have a period- $n$  cycle for all  $n > 3$  [6].

## 2.4 Noise

Papers on chaotic behavior often take a paradoxical approach to noise. One would think that sensitive dependence on initial conditions, the very heart of chaos, would amplify any external noise and obliterate the underlying behavior, yet many authors dismiss this issue almost out of hand. The explanation centers on the denseness with which chaotic trajectories cover the attractor densely. Noise bumps a point onto a nearby trajectory *where it would eventually end up at some point in the system's evolution anyway*. Noise does not change the character of the attractor, it just changes the order in which the whorls are traced out. An apt analogy is that "it gives one more shuffle to a well-shuffled deck of cards[12]." The attractor is bounded in space, due to the nonlinear folding illustrated by Smale's horseshoe, so the nonlinear amplification doesn't get out of hand. The Beta-shadowing theorem formalizes the statement: "With high probability, the sample paths of the problem with external noise follow *some* orbit of the deterministic system closely[8]." The Ruelle-Takens-Newhouse scenario uses this reasoning to sweep noise under the rug.

Information theory leads to another interesting approach. It has been noted [19] that the amount of information lost per iteration is  $\frac{\lambda}{bits}$ , where  $\lambda$  is the now-familiar Lyapunov exponent and *bits* is the number of bits needed to store the information. By definition — finite-precision computer arithmetic or Heisenberg uncertainty principle — initial conditions cannot be specified to infinite precision and chaos spreads this finite-width initial value band over the entire attractor after  $\frac{bits}{\lambda}$  iterations (see [3, page 52].) Noise has the same effect as imprecise specifications. Of course, if the band straddles some basin boundary, the repercussions will be global and related only to the probabilistic description of the noise or to the way the computer truncates numbers, not to the system's dynamics. This is where the "with high probability" part of the Beta-shadowing theorem breaks down. Basin boundaries can be very complicated — even fractal — and so can occupy much of the phase space. Systems where this occurs are pathologically sensitive to noise.

Noise on the output of an amplifier is not as much of a problem as noise on its input, but can still obscure measurements. On a calculator with six decimal places, two of which are obscured by numerical noise, solutions that cycle between 1.000002 and 1.000007 are indistinguishable, nor will the calculator find the predicted solutions if parameter values are entered that differ only by 0.00001 and are above and below some high-order bifurcation. The constant  $\kappa$  embodies this in the Feigenbaum scenario: the noise must have a  $\kappa$ -times smaller variance for one more bifurcation to be visible.



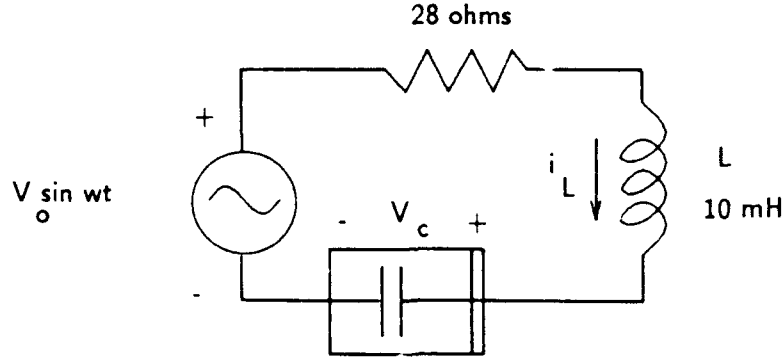


Figure 21: Nonlinear Oscillator Circuit

### 3 Applications — Nonlinear Oscillator

Testa *et al* [32] analyze a nonlinear oscillator, shown in figure 21, consisting of a series RLC circuit driven by a sine wave source. The capacitor in this circuit is actually a 1N953 varactor, which acts like a diode under forward bias and like a nonlinear capacitor under reverse bias, with

$$C \approx \frac{C_0}{\sqrt{1 + \frac{V_C}{0.6}}} \quad (8)$$

The differential equation for the system is:

$$L \frac{di_L}{dt} + Ri_L + \frac{C_0}{\sqrt{1 + \frac{V_C}{0.6}}} \frac{dV_C}{dt} = V_0 \sin 2\pi ft \quad (9)$$

The voltage-controlled capacitor makes the equations nonlinear and non-integrable. For low voltages, the square root term is close to one and the circuit acts like a linear RLC circuit, with a resonant peak at  $\omega_{res} = \frac{1}{\sqrt{LC}}$ . Testa *et al* give  $f_{res}$  as 93 kHz, but the component values given in the paper suggest  $f_{res} = 91.9$  kHz. As  $V_0$  increases, the nonlinear capacitance shrinks and  $f_{res}$  rises.

In these experiments,  $V_0$  is the nonlinearity parameter and  $V_C$  is the system state. The former is varied to generate a bifurcation diagram (with

| Periods | $V_0$ | Feigenbaum's Prediction |
|---------|-------|-------------------------|
| 2       | 0.639 | -                       |
| 4       | 1.567 | -                       |
| 8       | 1.785 | 1.766                   |
| 16      | 1.836 | 1.832                   |
| 32      | 1.853 | 1.847                   |

Table 2: Observations and Predictions

$V_C$  on the y-axis) and a spectrum (with the frequency of  $V_C$  on the y-axis) for the circuit. The authors deal with the one additional variable, the voltage source frequency, by fixing it near  $f_{res}$ . This decision is discussed later in this section. Generation of the bifurcation graph required a window comparator and simultaneous x and y sweeping of the scope beam (with  $V_C$  and  $V_0$ , respectively.)

The data resemble the bifurcation map for the logistic map (equation (6)). The first five period doublings, given in table 2, match Feigenbaum's predictions quite well. The intervals approach a limit at  $V_0 = 1.856$ , the onset of chaos. Beyond this threshold, windows of order appear within the chaos, all with periods that are a multiple of three (again, see [35].) Also apparent is the "veiled structure" of the attractors seen in cross section and the band-merging of reverse bifurcation. The frequency spectrum, taken just below the onset of chaos, also matches the Feigenbaum scenario very well. Peaks appear at the fundamental and its subharmonics. All but one of their heights match the predictions made in [8] and in [10].  $\kappa$ , the measure of "how much noise is required to obliterate a bifurcation," also correlates well with Eckmann's predictions (6.3 measured, 6.62 predicted.)

Two things are troubling about this paper. First of all, the authors fix the driving frequency of a resonant circuit without giving any explanation. Some discussion of why a value "near  $f_{res}$ " was chosen and how behavior changes with frequency would seem necessary; electronic circuit models can be drastically different at high and low frequencies. Judging by an unsuccessful attempt to build the circuit and reproduce the experiment, it would seem that the choice was not at all arbitrary. No period doubling and no chaos were observed. The behavior was exquisitely frequency dependent, due to the nonlinearity and the high  $Q$ . At low frequencies, the capacitor volt-

age does indeed do odd, nonlinear things as the source voltage is turned up, but *harmonics*, not subharmonics, appeared. Above  $f_{res}$ , the system looks more linear (mainly because the rolloff lowers the amplitude and anything looks linear in small enough increments.) Slightly different component values were used ( $L = 10$  mH,  $R = 27 \Omega$  and a “varactor” — the collector/base junction of a 2N6193 power transistor — with a slightly smaller  $C_0$ ) than those given in [32]. It is quite likely that this system is so sensitive to equation coefficients that these slight changes pushed the period doublings and chaotic behavior right off the observable voltage scale, or even forced the system into a non-chaotic zone. The driven damped pendulum, governed by an almost-identical equation, is extremely sensitive to the drive: its parameter space (drive frequency vs. amplitude) is honeycombed with zones of order and chaos[7]. If the experiment is so ticklish as to preclude repetition, then the authors should either say so or explain why the chosen parameters cause chaotic behavior when other nearby parameters do not (as given, for example, in [7].)

Secondly, the authors “assume a correspondence between [the oscillator and the logistic map]”, down to the details of equating  $V_0$  with  $K$  and  $V_C$  with  $x$ , again without explanation. The universality of chaos may be the answer: “As long as the model is in the same universality class as the real system, both will undergo a period doubling sequence... This means that we can get the right physics out of very crude models... [5]” It is not obvious why this oscillator and the logistic map are in the same universality class (loosely, this means that they have the same number and power of terms in their power series.) Some formal justification seems warranted. The fragility of this correspondence is illustrated by comparisons between oscillator data and logistic map prediction for  $\delta$ : deviations ranged from 10% to 30%. Comparisons to Feigenbaum’s  $\alpha$  and  $\epsilon$  and Eckmann’s  $\kappa$ , only had 3%, 4% and 4% error (respectively). These numbers also come from an approximation, but it is obviously a better one.

This experiment clearly fits into the Feigenbaum scenario because its bifurcations follow the pattern defined by  $\alpha$ ,  $\epsilon$  and  $\kappa$ . It does not fit the Ruelle-Takens-Newhouse scenario — too many spikes appear before the onset of chaos. It is impossible to determine its match with the Pomeau-Manneville scenario; there may well be one or more saddle-node bifurcations, but none were captured in the published data. Another paper on this subject by these authors does present observations of such a bifurcation[27].

## 4 Applications — Belousov-Zhabotinskii Reaction

The Belousov-Zhabotinskii reaction is one of the most colorful examples in nonlinear dynamics<sup>8</sup>. As five chemicals — ferroin, malonic acid, sodium bromate, sulfuric acid, and cerous ion — are injected into a reactor, concentrations of different brightly colored ions vary chaotically in space with time and injection rate<sup>9</sup>. This experiment is different from many others in the chaos literature in that it is not easily repeatable with a computer, a box of resistors, or a dripping faucet; [29] gives the recipe, but cautions “Perhaps the mathematical reader should be warned that diluting sulfuric acid produces heat...”

The parameters of this experiment are best described by analogy to the nonlinear oscillator of the last section. The sine wave source is equivalent to the injected chemicals; the nonlinearity parameter of voltage amplitude is replaced by “residence time”, which is directly related to injection rate. Dissipation, provided by the oscillator’s resistor, manifests here as the continual consumption of the reactants. Finally, system behavior is measured not in voltages but in ion concentrations at a point in space.

Hudson and Mankin [19] present ion concentration data at three residence times. Two of these data sets show periodic behavior and one is chaotic. The authors’ stated purpose is not to trace the path to chaos, but simply to prove that the apparently aperiodic behavior that was observed is indeed chaotic. They do mention that period doublings occur as the nonlinearity (residence time) is turned up, eventually resulting in semi-random behavior, but this issue is pursued no further.

Almost all of the tools introduced in sections 1 and 2 are used in [19]. Ion concentrations are plotted against time, frequency, each other, their derivatives and their delayed values. The two latter cases require some justification, as derivatives and delayed values are in some sense “manufactured variables.” They are, however, *independent* variables; for a  $n^{\text{th}}$ -order system, the use of any  $n$  independent quantities uniquely specifies the behavior. An  $n$ -dimensional state space can even be reconstructed from a single stream of time-series data gathered at a single point[9]. Using a different set of  $n$  variables simply brings out a different view of the state space.

---

<sup>8</sup>Excepting computer graphics.

<sup>9</sup>The ferroin serves only to bring out the colors, so it is omitted from serious studies like [19].

At low residence time, the phase space and time domain plots of the bromine ion concentration show period-two oscillations. At a higher injection rate, the plots are aperiodic and a strange attractor takes form on the phase plot. One final, higher value puts the system into a period-three window in the chaos band. The origin of the second column of phase plots in figures 3 and 4 of [19] is a mystery; the authors refer only to plots of a single quantity (Br-). Perhaps the other column shows data for the other ion (Pt+)?

The frequency spectra of these three concentrations look qualitatively different from those measured in turbulence or electronic experiments: both background noise and the broad-band noise that accompanies chaos are quite frequency-dependent. This is not addressed and may be due to the probes used to gather the data. The authors' viewpoint on this noise is also qualitatively different. They speak of frequency peaks *disappearing* with the onset of chaos where Eckmann and others note the appearance of broad-band energy which *obscures* the peaks. The tips of the peaks are still visible in the chaotic ion concentration data, so the latter description seems more appropriate.

The second half of the paper concentrates on the chaotic data set. A transformation on the phase space, of the type discussed in a previous paragraph, is performed and some very tentative conclusions are drawn from the attractor's shape on the new axes. The return map<sup>10</sup> (see figure [14]) is plotted for a particular cross section of the phase space and is analyzed in depth. The authors present results of a complicated curve-fitting procedure, used to compute the Lyapunov exponents of that return map.  $\lambda$ s are invariant (a return map from a different cross section would have the same  $\lambda$  [5, page 11]) and, as mentioned before, are direct indicators of chaos. For the data set under consideration,  $\lambda = 0.62$ . This value is extremely sensitive to the parameters of the curve fit. The authors convey this concept in an interesting way, varying these parameters and generating a matrix of  $\lambda$ s. One quarter of the values turned out negative, so slight changes in the return map could result in periodic flow (cf. the frequency dependence of chaos in the circuit in section 3.) Finally, sensitive dependence upon initial conditions is illustrated by tracing the path of iterates from a narrow band of initial values to a chaotically-distributed batch of points on an attractor (much like the figure on page 52 of [3]).

For a variety of reasons, it is difficult to fit this experiment into one of Eckmann's slots. The authors do not present a series of snapshots of the system as it enters chaos. They do allude briefly to chaos following upon the heels of period-doublings, but they do not discuss the mechanism of

---

<sup>10</sup>Hudson and Mankin's terminology is confusing; this is called a "next-amplitude map" in their introduction and a "return map" for the rest of the paper.

the transition — they give only a description of the finished product. The frequency spectra do not match any of those given in [8]. The frequencies do not appear to be independent and yet they don't follow the Feigenbaum subharmonic sequence. The heights of the peaks seem to fall off smoothly, as opposed to the sawtooth pattern defined by  $\delta$  and  $\epsilon$ . This pattern is unique among the papers reviewed for this paper; another paper on the same reaction [28] seems to show frequency peaks in the Feigenbaum sequence, but the scale only includes a few bifurcations. This may indicate an entirely different path to chaos.

## 5 Applications — Solar System

“Solar system dynamics encompasses the orbital and rotational dynamics of the planets and their natural satellites, the coupling between them, and the slow evolution of the orbits and spins due to tidal friction. It is primarily the dynamics of resonances, and resonances are almost always associated with chaotic zones.” [34]

Chaos in the solar system should be of absolutely fundamental interest to its denizens. From an experimental standpoint, this system is very different from an RLC circuit or chemicals in a vat, and not just because of size. Time scales are vastly longer than in the previous two examples. The tools of choice are plots in the phase space and the time domain. Except for tidal friction and the occasional collision, dissipation does not exist. (Recall that dissipation is not a necessary condition for chaos, just for the existence of attractors.) The time scales of these exceptions are so different from the others in the system that they are treated as perturbations. The tides may be thought of as causing objects to wander slowly across the phase plot of the non-dissipative system, rather than as causing the phase plot to evolve with time. Because the system is so large and complicated, many more forces have first or second order effects on the solution than in electronics, fluid dynamics or chemistry problems, so approximation accuracy is very important.

One example where modeling is extremely important is the chaotic rotation of Hyperion, one of Saturn's moons. Any aspherical satellite is subject to restoring torques which try to synchronize the spin with the rotation — hence the “dark side of the moon”. Tidal forces also align the spin axis, the largest moment of inertia, and a vector perpendicular to the plane of orbit. Wisdom used this alignment as an assumption in the first-order model in [34]. The resulting equation cannot be solved in closed form: the time dependence of the torque, caused by Hyperion's highly eccentric orbit, makes

it non-integrable<sup>11</sup>. Numerical integration yields a complicated phase diagram, plotted in the phase space of angular velocity versus angular position, showing a large chaotic region dotted with periodic islands. The orbit was sampled at periapse, the point of closest approach to Saturn. The islands correspond to resonances like the spin-lock of earth's moon.

This model cannot account for chaotic *tumbling* because one of its assumptions was to fix the spin axis relative to the plane of orbit. If this condition is relaxed, the spin axis is found to be wildly attitude-unstable on the largest periodic island, the large central chaotic zone and on most of the smaller islands as well. If Hyperion's spin axis is just slightly off perpendicular when it enters any of those regions, the satellite will tumble chaotically. The equations are so complicated that Wisdom resorts to Lyapunov exponents — positive in three of the six phase space dimensions (The Euler angles  $\theta$ ,  $\phi$ ,  $\psi$  and their derivatives) — to affirm his diagnosis of chaos.

The evolution scenario suggested by this model is fascinating: over the age of the solar system, tidal forces slowed the satellite's chaotic spin and aligned its longest axis perpendicular to the orbital plane, then "the work of the tides over aeons was undone in a matter of days" when Hyperion entered one of the attitude-unstable areas with its axis just off center and started the cycle over again. This hypothesis was verified by Voyager photographs, which showed the satellite in a position "inconsistent with other known regular rotation states."

The attitude instability of the large synchronous island is unique to Hyperion, so the other moons in the solar system don't tumble chaotically. However, many of them did in the past, because (due to a theorem, proposed by Kolmogorov and proved by Arnold and Moser, called the KAM theorem) almost all resonances — islands on surfaces of section which correspond to stable orbits — are surrounded by chaotic zones. The size of these zones depend both on deviations from spherical symmetry and on orbit eccentricity. Perfectly spherical satellites orbiting in perfect circles and other, less perfect bodies that happened to begin life in exactly the right spot did not have to traverse chaotic zones on the way their current stable synchronous islands, but all others did.

The orbit eccentricity distribution of the asteroids in the belt between Mars and Jupiter is not uniform. Gaps and enhancements in this distribution are found at resonance points with Jupiter, but the mechanism of their formation has never been adequately explained. The mathematics near such a resonance is complicated, so exact closed-form solutions have not been found. Numerical integration is prohibitively expensive because of the

---

<sup>11</sup>This implies that Hyperion could not act chaotically if it were in a circular orbit.

system's different time scales; one of the figures in [34] required 200 VAX hours to generate, even with significant effort devoted to accelerating the integrator. Because of this expense, earlier integrations were terminated after 10,000 years of apparent steady state behavior, having lulled investigators into a false sense of security. Wisdom's longer integrations, however, showed that systems can be well-behaved for millions of years, then come abruptly out of dormancy and into wild orbits which jump from one eccentricity to another. The erratic patterns of the data led him to suspect chaos and to assess it as a possible method for clearing the Kirkwood gaps. Numerical integrations for a typical asteroid near the 3/1 Kirkwood gap verify these suspicions. The intermittent behavior is explained by a strange chaotic band that has roughly constant eccentricity ( $e$ ) through most of its domain and a narrow thread extending out to much higher  $e$ s. Orbits with such high eccentricities cross the paths of Mars and the Earth. This hypothesis neatly dovetails the evacuation of the Kirkwood gaps and the origin of meteorites that strike the Earth. Experimental verification is extremely convincing — the boundaries of the calculated chaotic zone and the observed edges of the 3/1 gap overlap one another [34, figure 9].

Other resonance points do not yield such neat explanations, perhaps because their dynamics are more complicated. Two such cases are the Kirkwood gap at the 2/1 resonance and the enhancement (the Hilda group) at the 3/2 point. The Digital Orrery[1], a dedicated celestial mechanics multiprocessor, was used to integrate model equations for particles in these areas. These data showed previously unknown chaotic regions, one of which is near the 2/1 point. Chaotic behavior is not enough to explain the gap — the mechanism that actually destroys or removes the asteroids must be identified as well. Once again, a better model (allowing motion in all three dimensions) uncovered a possible mechanism — close encounters, or, more rarely, collisions with Mars. More recently[31], the Orrery was used to show that Pluto's orbit is chaotic, with  $\lambda \approx \frac{10^{-7.3}}{\text{year}}$ . Chaos is not the solution to all problems in dynamical astronomy, however. It did not explain the 3/2 enhancement, nor does it play an obvious role in the formation of the gaps in Saturn's rings.

What distinguishes this work from the other papers reviewed here is the reach of the conclusions drawn from the data. Eckmann waffles about "domain of applicability", Testa *et al* and Hudson and Mankin are content merely to show chaos' patterns in their experiments. Wisdom predicts and verifies real, far-ranging effects. As with the other applications, it is difficult to classify Wisdom's data within Eckmann's framework. The difficulty arises from the sheer complexity of the application, as well as from the inadvisability of "varying the nonlinearity parameters" of the solar system to watch the resulting behavior — we might vary ourselves right out of existence. *Model*



parameters can be varied to check extensions to hypotheses, as Wisdom did for differently-shaped moons, but deep changes in the equations might create nonphysical situations — and model verification for a hypothetical situation is impossible. The solar system does, however, contain many bodies in many stages of evolution, which in some sense comprise a set of “snapshots” like those in the previous application papers. Time, not nonlinearity, is the variable, so the “paths to chaos” that can be distilled out of this paper are time evolutions and not bifurcation diagrams. In spirit, Wisdom’s data resemble the frequency spectrum in [19] — a description of the finished product of chaos.

High-dimension, non-dissipative systems may not be in Eckmann’s stated domain, but some extensions of his classifications do apply. Feigenbaum’s scenario, in particular, has been extended to such systems by other authors [5]. The phase plot of Hyperion’s orbit shows nested island chains with two elements, the higher-dimensional analog to the first bifurcation (see [20, figure 5] or [16]), possible evidence that Feigenbaum’s period doubling is at work. Intermittent chaotic behavior is clearly present on the eccentricity-versus-time plots. It is attributed to slow tidal wandering in and out of different zones on the Hamiltonian (non-dissipative) phase plot — a possible extension of the ideas in the Pomeau-Manneville scenario.

None of the three applications reviewed fits neatly into one scenario. This is a consequence of incomplete theory and inexact data. The three scenarios do not cover all possibilities — indeed, that was one of Eckmann’s disclaimers. This is highlighted in the chemical reaction of section 4, where the clearly chaotic experimental data fit none of the specified patterns. Even when the data do fit the patterns, formal, exhaustive verification of a scenario’s “if” clause is impossible. Distinguishing between several closely-related types of bifurcations (Hopf, pitchfork, inverse saddle-node) is not experimentally practical. More useful definitions would emphasize distinctive, observable characteristics, rather than mathematical details (the latter are important, but not in classifying experimental data.) A broader definition, in which the three scenarios described are simply special cases of a common whole, would be extremely valuable. The universality of chaos does suggest that such a broad definition exists, even if it has not yet been discovered.

## 6 Universality in Chaos

Chaos is universal in that a great many systems act alike when their nonlinearities are turned up. The distinctive patterns of period doubling, broad-

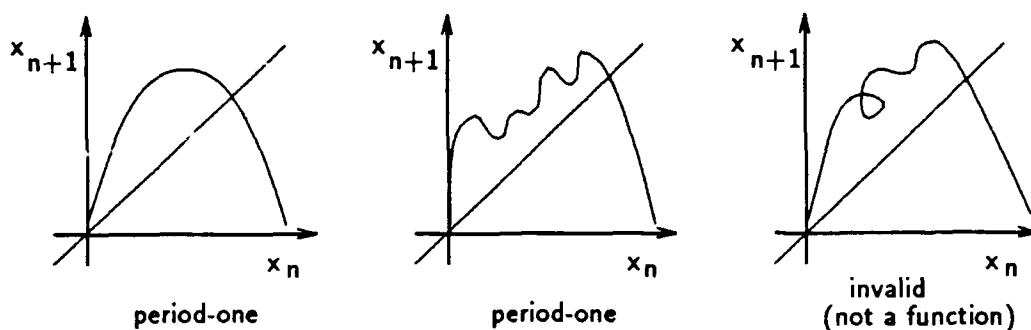


Figure 22: Return Maps With Slope=1 at the 45 Degree Line

band “noise” — that isn’t really noise — and strange attractors have been found in an incredible variety of man-made and natural systems. Identification of these new patterns has changed experimental methods; noisy or random data now warrants a second look.

The mathematics behind this universality is exact — chaos theory is not just a “better linearization.” This exactness causes many papers in the field to read like topology texts. Armed with such formalism, however, those papers are able to prove sweeping results like Sarkovskii’s theorem (page 21), which define existence and ordering of periods, chaotic bands and windows of order. Most of the proofs hinge only on a function’s slope at one point or the nature of its maximum, e.g., “The order [of the windows] does not depend on the map  $f(x)$ , as long as  $f$  has a differentiable maximum and falls off monotonically...” [5]. Looking back at the return map, one can see why this small set of requirements leads to universality. Recall that a bifurcation occurs when the slope of the curve reaches 1 at the 45 degree line. This is a *local* consideration. It doesn’t matter (within limits) what the curve does anywhere else. See figure 22. Also, on a small enough scale, any curve looks like a straight line: “After we have magnified the neighborhoods of fixed points many times, practically all information about the global shape of the starting function  $f$  is lost, and we are left with a universal function  $g(x)$  [5].” At first, Feigenbaum thought that period doubling was a particular property of the logistic map. It was only after he found doubling in the equation

$$x_{n+1} = \lambda \sin \pi x_n,$$

with the same  $\delta$ , that he broadened the domain of the theory. One of the less topologically rigorous papers puts it thus: “Around the maximum, it

looks like a parabola...like any sensible approximation to a function with a hump[5]." Implicit in the use of the word "sensible" is the breadth of the universality class. Chaos lets one predict something about the behavior of systems in this class without analyzing unsolvable  $n^{\text{th}}$  order differential equations.

This universality makes the theory *useful*; knowing chaos' precursors could help one head it off[18] or encourage it[2], as desired. Universality also makes the theory widely applicable. "Dynamical disease"[24] manifests in physiological rhythms in time or space; presence or absence of chaos in these rhythms can be significant. An EEG of a healthy brain is chaotic, for example, while an epileptic brain is often quasiperiodic. The human heart is normally periodic, but can go into a chaotic fibrillation state. Chaos theory might allow construction of a better model for the heart, which could be studied with changing nonlinearity (adrenaline, blood supply...) A better pacemaker might sense period doubling or other precursors to chaos and administer a slight shock to divert its onset, a less traumatic technique than the current full phase reset after onset of arrhythmia. The dynamics of a driven oscillator, like the RLC circuit in section 3, give insight into the interactions of a mechanical ventilator and a person's normal breathing rhythm. A more global example is the earth's magnetic field, which reverses now and then. Researchers are trying to find the "attractor" and understand the behavior. Note that, even if the attractor were known, the date of the next reversal could not be predicted because exactly what comprises "initial conditions" is unknown, nor could they be measured to infinite precision if they were known.

The richness of structure that chaos stirs up in simple systems suggests a way to classify complex behavior. Presented with figure 23, any chaos devotee would immediately recognize the Mandelbrot set and give the system equation

$$z_{n+1} = z_n^2 + c$$

which is a lot more compact than the figure. Genetics is a less trivial example. Genes are vastly less complex than the structures that they generate. Nonlinear dynamics does not give the "equations" — the genetic encoding — but it does suggest a mechanism that can bridge the gap. This compression and expansion of information resembles the operation of companders in communications. If information happened to come in Mandelbrot sets, one could just transmit " $z_{n+1} = z_n^2 + c$ " and the appropriate  $c$ , then reconstitute the information at the other end of the channel. Cryptography is another possible application. A few times through an iterative chaotic map would certainly scramble data quite well, but even a single bit of noise would devastate the decoding process.

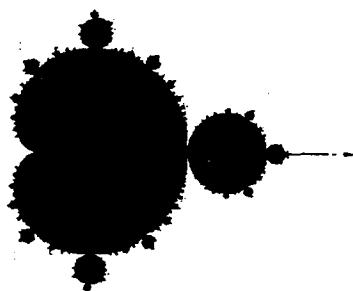


Figure 23: A Set in the Complex Plane

Although chaos does simplify explanations for some systems that once were thought to be random or too complex to describe, the predictions it lets us make about those systems are limited. This dooms it as a tool for playing the stock market [20] or roulette (one of the primary projects of the Dynamical Systems Collective at Santa Cruz<sup>12</sup>.) It also vindicates Lorenz, its discoverer, and verifies what meteorologists have always known — weather is fundamentally unpredictable.

---

<sup>12</sup>These projects are also doomed for another reason...even if the initial conditions were known. Roulette wheels and stock markets are their own fastest simulators.

## A The Van der Pol Oscillator

The Van der Pol oscillator is an RLC circuit whose nonlinear resistor looks negative for small voltages and positive for large voltages. An RLC with a positive  $R$  has an unstable equilibrium point at the origin of its state space plot, surrounded by growing spirals. In an RLC circuit with a negative  $R$ , the fixed point is stable and the spirals decay in towards the origin. The nonlinear Van der Pol resistor acts as a restoring force, forcing the voltage to a limit cycle between the two domains. The radius of the limit cycle can be approximately calculated by equating the power absorbed by the system when the resistor is acting negative and the power generated when the resistor is acting positive. The circuit and the nonlinear resistance curve are shown in figure 24. The state equations are:

$$\begin{aligned} i_L' &= \frac{-(v_C + ai_L - bi_L^3)}{L} \\ v_C' &= \frac{i_L}{C} \end{aligned}$$

The Jacobian  $\mathcal{J}$  is:

$$\begin{bmatrix} -\frac{a-3bi_L^2}{L} & -\frac{1}{L} \\ \frac{1}{C} & 0 \end{bmatrix}$$

The eigenvalues of  $\mathcal{J}$  — the natural frequencies of the circuit — are the roots of:

$$|\lambda I - \mathcal{J}| = 0$$

which are:

$$\lambda = \frac{3bi_L^2 - a}{2L} \pm j\sqrt{\frac{1}{LC} - \frac{(a - 3bi_L^2)^2}{4L^2}}$$

The limit cycle is shown in figure 25. It is almost circular, but not quite; the slope of  $v_R$  at the origin causes some harmonic distortion. A more complex resistor can give the circuit more than one attractor, separated by a metastable "separatrix." See figure 26.

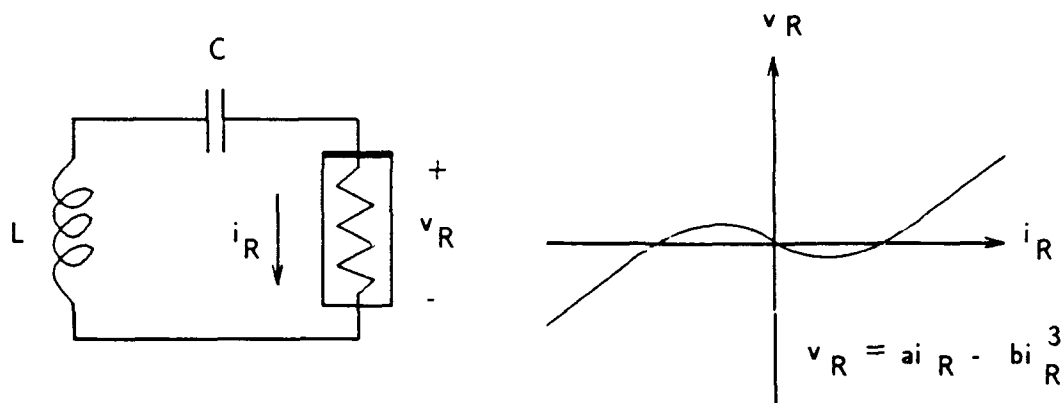


Figure 24: Van der Pol Oscillator

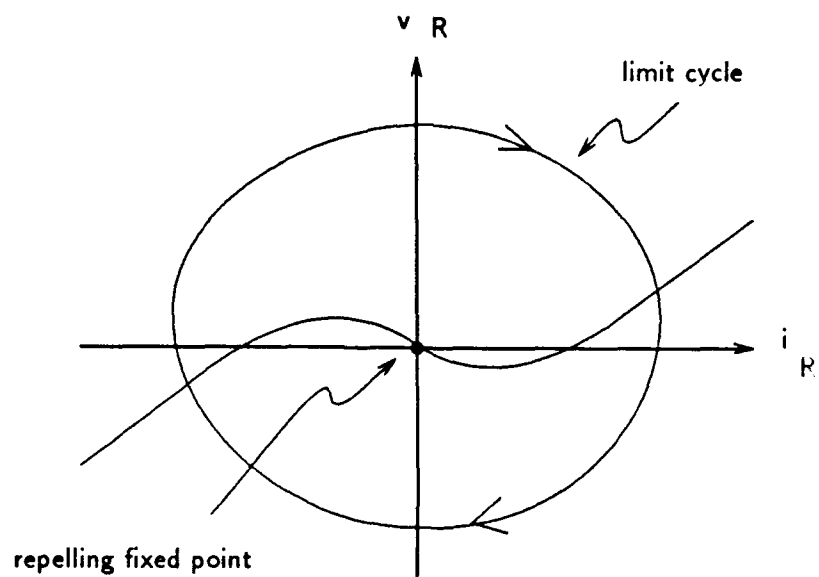


Figure 25: Limit Cycle

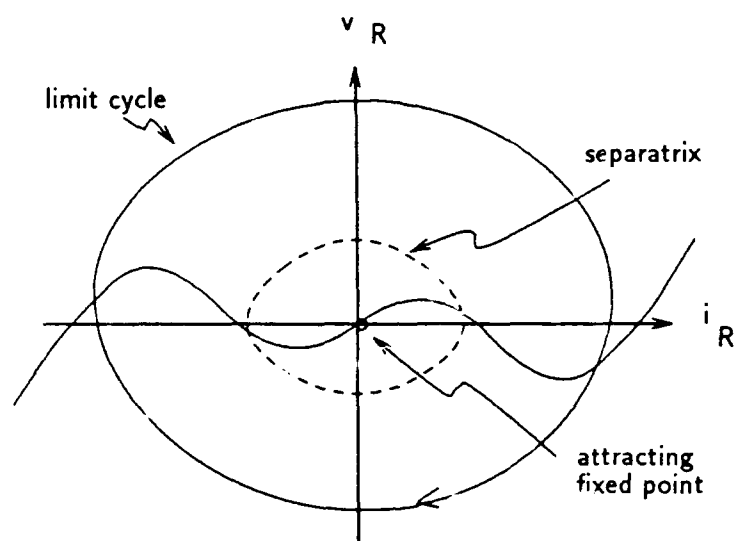


Figure 26: A More Complex Resistor and the Resulting Limit Cycle

## B The Hénon Attractor

For some parameter values, iterates of the system of nonlinear difference equations:

$$\begin{aligned}x_{n+1} &= 1 - \alpha x_n^2 + y_n \\ y_{n+1} &= \beta x_n\end{aligned}\tag{10}$$

form strange attractors in correlation space (cf. figure 16.) Figure 5 in the introduction shows plots for  $\alpha = 1.2$  and  $\beta = 0.4$ ; plots for several other parameter values are shown in figure 27. The attractor mutates as the parameters change — for the lowest  $\alpha$  values in the figure (top left), the attractor is actually a period-4 cycle. Raising  $\alpha$  induces a bifurcation to a period-8 cycle. Higher  $\alpha$ s force the system into a chaotic zone at which point the Lyapunov exponent becomes nonzero. In general,  $\lambda$  increases with increasing  $\alpha$  or  $\beta$  until  $\alpha = 1.24, \beta = 0.4$ . Any increase beyond this point results in an unstable system and diverging iterations.

Hénon's goal, in [17], was to find the simplest system that exhibited the behavior observed in Lorenz' work on the Navier-Stokes equations (see figure 1.) The latter are differential equations, but they can be modeled by difference equations — which require orders of magnitude less time to evolve with a computer. Hénon never claims that this set of equations models any particular physical system, but many other authors have noted that correlation plots of physical data from dripping faucets look very much like Hénon's pictures. Formal justification of this conjecture would require determining the differential equations for a drip forming at an orifice, followed by application of numerical integration methods, like Forward Euler or Runge-Kutta, and identification of equations (10) in the results. The fluid dynamics of such a drip is horribly complicated and the stability of the equations is structurally sensitive to model parameters. Another approach [30] is to use a simpler model of the system, shown in figure 28. The mass grows with time, forcing the spring to stretch out and lowering the frequency of any oscillations that are present. When the mass reaches  $x_{crit}$ , a portion breaks off. To make the equations non-integrable, the amount that breaks off must be a function of velocity. However, this introduces a singularity into the equations, which precludes any use of methods like Forward Euler and symbolic recovery of equations (10).



One can solve this system in pieces by numerically integrating the equations:

$$\begin{aligned}\frac{dx}{dt} &= v(t) \\ \frac{dv}{dt} &= -\frac{k}{m(x, v, t)}x(t) \\ \frac{dm}{dt} &= h\end{aligned}\tag{11}$$

where  $x$  is the position of the mass,  $v$  the velocity,  $k$  the spring constant, and  $h$  the (linear) rate of growth of  $m$ . When  $x$  reaches  $x_{crit}$ , the time is recorded and the integration is restarted with a new value for the mass, as dictated by the velocity at  $x_{crit}$ . A sample run is shown in figure 29. The top line is  $x$ , the middle  $v$  and the bottom  $m$ . If the intervals between break-offs are plotted in correlation form, the resulting plot (figure 30) does indeed "look like" Hénon's pictures: suggestive but not conclusive evidence that the latter are a good model for the former, at least for some values of  $\alpha$  and  $\beta$ .

#### Acknowledgements

Randy Fenstermacher and Ken Yip helped me clear up many conceptual problems and misunderstandings. Peter Nuth and Gerry Sussman made proofreading comments which helped form the substance and organization of this paper and Natalie Tarbet's knowledge of the English language made it a lot more readable. Arthur Gleckler wrote the program that generated the picture of the Mandelbrot set on page 34. This report describes research done at the Artificial Intelligence Laboratory of the Massachusetts Institute of Technology. Support for the laboratory's artificial intelligence research is provided in part by the Advanced Research Projects Agency of the Department of Defense under Office of Naval Research contracts N00014-85-K-0124 and N00014-86-K-0180.

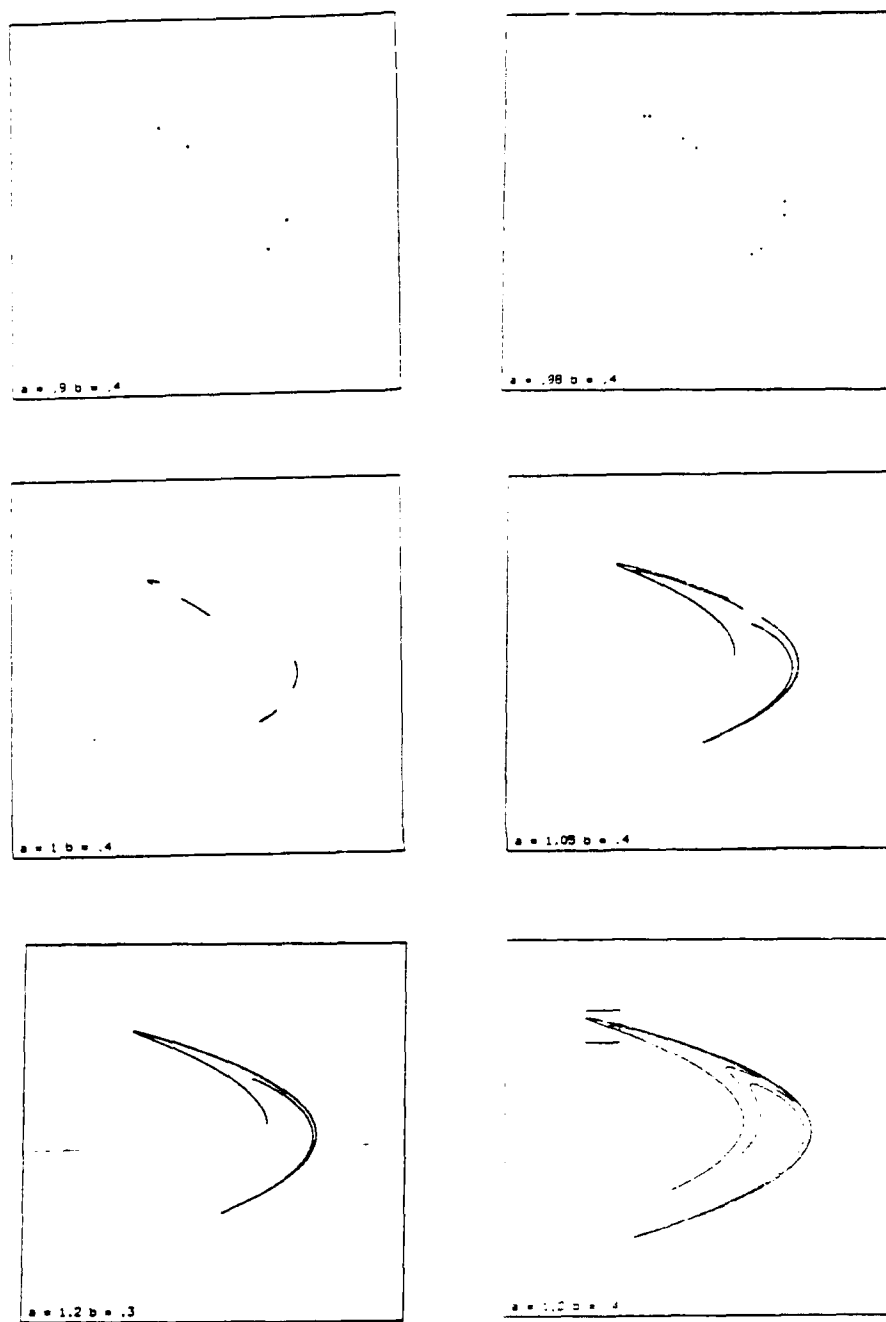


Figure 27: Iterations of Hénon's equations in Correlation Form

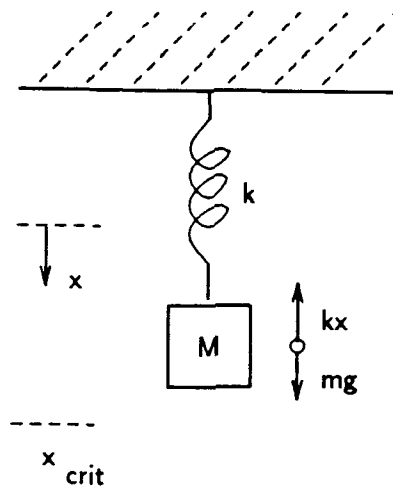


Figure 28: Model for a Dripping Faucet

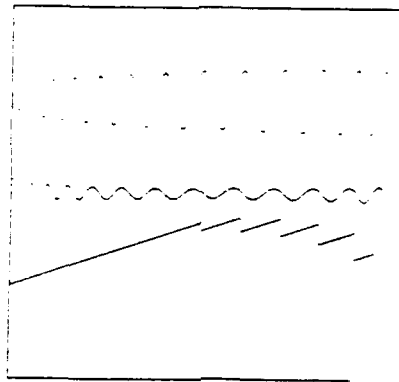


Figure 29: Numerical Integration for the Model

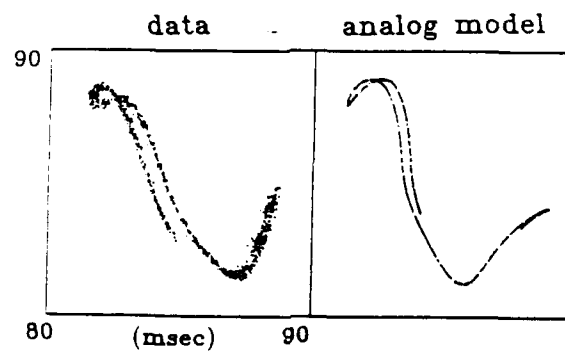


Figure 30: Plots for Model and Real Data (from (30))

## References

- [1] Applegate, J. F. et al, "A Digital Orrery", *IEEE Transactions on Computers*, September 1985.
- [2] Bradley, E., "Taming Chaotic Circuits," PhD Thesis Proposal, MIT Artificial Intelligence Lab, May 1990.
- [3] Crutchfield, J. P. et al, "Chaos", *Scientific American*, December 1986.
- [4] Collet, P. et al, "Period Doubling Bifurcations for Families of Maps on  $R^n$ ", *Journal of Statistical Physics*, **25**, 1981.
- [5] Cvitanovic, P., *Universality in Chaos*, Introduction, Adam Hilger (Bristol U.K.), 1984.
- [6] Devaney, R. L., *An Introduction to Chaotic Dynamical Systems*, Benjamin/Cummings (Menlo Park, CA), 1986.
- [7] D'Humieres, D. et al, "Chaotic States and Routes to Chaos in the Forced Pendulum," *Physical Review A*, **26**, 3483(1982).
- [8] Eckmann, J-P., "Roads to Turbulence in Dissipative Dynamical Systems", *Reviews of Modern Physics*, **53**, 1981.
- [9] Farmer, J.D. and J.J. Sidorowich, "Exploiting Chaos to Predict the Future and Reduce Noise," in Y.C. Lee, editor, *Evolution, Learning and Cognition*, World Scientific, 1988.
- [10] Feigenbaum, M. J., "Universal Behavior in Nonlinear Systems", *Los Alamos Science*, **1**, 1980.
- [11] Ford, J. et al, "On the Integrability of the Toda Lattice", *Progress of Theoretical Physics*, **50**, 1973.
- [12] Gleick, J., *Chaos*, Viking, 1987.
- [13] Goldstein, H., *Classical Mechanics*, Addison-Wesley (Reading, MA), 1980.
- [14] Grebogi, C. et al, "Chaos, Strange Attractors and Fractal Basin Boundaries in Nonlinear Dynamics", *Science*, **238**, 1987.
- [15] Grebogi, C. et al, "Controlling Chaos" in *Chaos: Proceedings of a Soviet-American Conference*, American Institute of Physics, 1990.

- [16] Helleman, R. H. G., "Self-Generated Chaotic Behavior in Nonlinear Mechanics", *Fundamental Problems in Statistical Mechanics*, **5**, 1980.
- [17] Hénon, M., "A Two-dimensional Mapping with a Strange Attractor", *Communications in Mathematical Physics*, **50**, 1976.
- [18] Hogg, T. and B. Huberman, "Controlling Chaos in Distributed Systems," Submitted to *IEEE Special Issue on Distributed Artificial Intelligence*, 1990.
- [19] Hudson, J. L. and J. C. Mankin, "Chaos in the Belousov-Zhabotinskii Reaction", *Journal of Chemical Physics*, **74**, 1981.
- [20] Jensen, R. V., "Classical Chaos", *American Scientist*, March 1987.
- [21] Kuhn, T. H., *The Structure of Scientific Revolutions*, University of Chicago Press, 1970.
- [22] Landau, L. and E. Lifschitz, *Fluid Dynamics*, Pergamon, 1959.
- [23] Lorenz, E. N., "Deterministic Nonperiodic Flow", *Journal of the Atmospheric Sciences*, **20**, 1963.
- [24] Mackey, L. and M.C. Glass, *From Clocks to Chaos: The Rhythms of Life*, Princeton University Press, 1988.
- [25] Mandelbrot, B. B., *The Fractal Geometry of Nature*, W. H. Freeman, N.Y., 1983.
- [26] Peitgen, H-O. and P. H. Richter, *The Beauty of Fractals*, Springer-Verlag, 1986.
- [27] Perez, J. and C. Jeffries, "Direct Observation of a Tangent Bifurcation in a Nonlinear Oscillator", *Physics Letters*, **92A**, 1082.
- [28] Roux, J. C. et al, "Representation of a Strange Attractor from an Experimental Study of Chemical Turbulence", *Physics Letters*, **77A**, 1980.
- [29] Ruelle, D., "Strange Attractors", *The Mathematical Intelligencer*, **2**, 1980.
- [30] Shaw, R., *The Dripping Faucet as a Model Chaotic System*, Santa Cruz: Aerial Press, 1984.
- [31] Sussman, G.J. and J. Wisdom, "Numerical Evidence That the Motion of Pluto is Chaotic," *Science*, **241**, 433(1988).

- [32] Testa, J. *et al*, "Evidence for Universal Chaotic Behavior of a Driven Nonlinear Oscillator", *Physical Review Letters*, **48**, 1982.
- [33] Thompson, J. M. T. and H. B. Stewart, *Nonlinear Dynamics and Chaos*, Wiley, 1987.
- [34] Wisdom, J., "Chaotic Behavior in the Solar System", *Nuclear Physics B*, 1987.
- [35] Yorke, J. A. and T-Y. Li, "Period Three Implies Chaos", *American Mathematics Monthly*, **82**, 1975.